Supporting information

Conjugating AIE-featured AuAg nanoclusters with highly luminescent carbon dots for improved visible-light-driven antibacterial activity

Naiwei Liu,[†a] Yichun Wang,[†a] Ziping Wang,[b] Qiuxia He,[a] Yong Liu,[a] Xinyue Dou,[a] Zhengmao Yin,[a] Yang Li,[c] Haiguang Zhu,[a] and Xun Yuan*[a]*

[a]College of Materials Science and Engineering, Qingdao University of Science and Technology (QUST), 53 Zhengzhou Rd., Shibei District, Qingdao 266042, P. R. China. Email address: zhuhg@qust.edu.cn (H. Zhu), yuanxun@qust.edu.cn (X. Yuan)

[b]Weifang University of Science and Technology, Shandong Peninsula Engineering Research Center of Comprehensive Brine Utilization, Weifang 262700, P. R. China.

[c]Jiangsu Key Laboratory of Micro and Nano Heat Fluid Flow Technology and Energy Application, School of Physical Science and Technology, Suzhou University of Science and Technology, Suzhou 215009, P. R. China.

† These two authors contributed equally to this article.

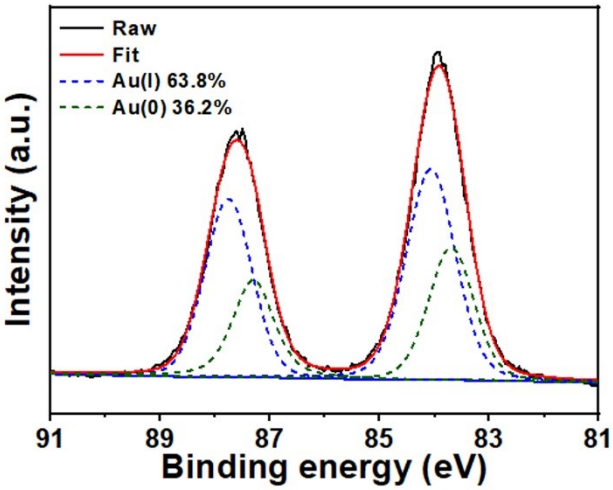

Figure S1. High-resolution XPS spectrum of Au_{4f} in the AIE-featured AuAg NCs.

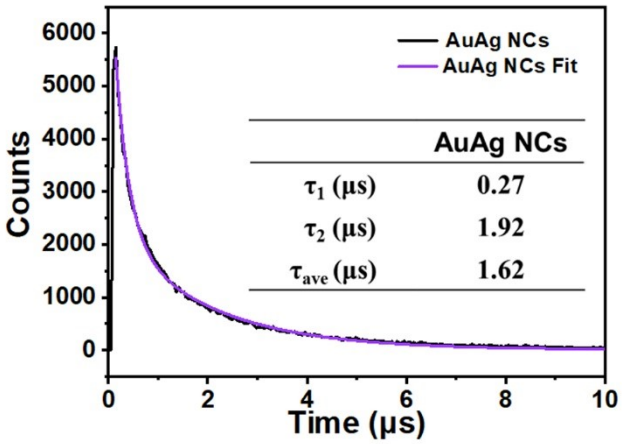

Figure S2. PL decay profile and corresponding exponential fit of the AuAg NCs. Inset: the calculated PL lifetimes of τ_1, τ_2 and τ_{ave} (average luminescence lifetime).

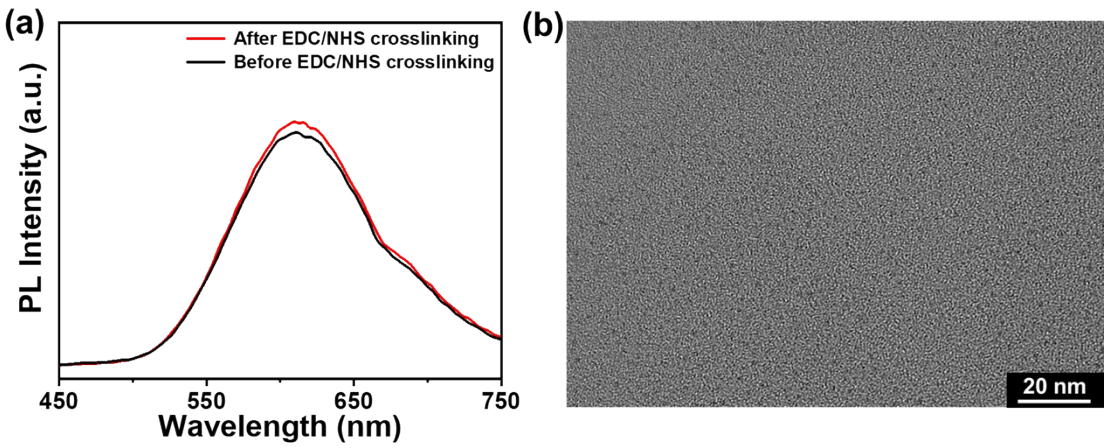

Figure S3. (a) The PL emission spectra of AuAg NCs before and after EDC/NHC crosslinking. (b) TEM image of AuAg NCs after EDC/NHC crosslinking.

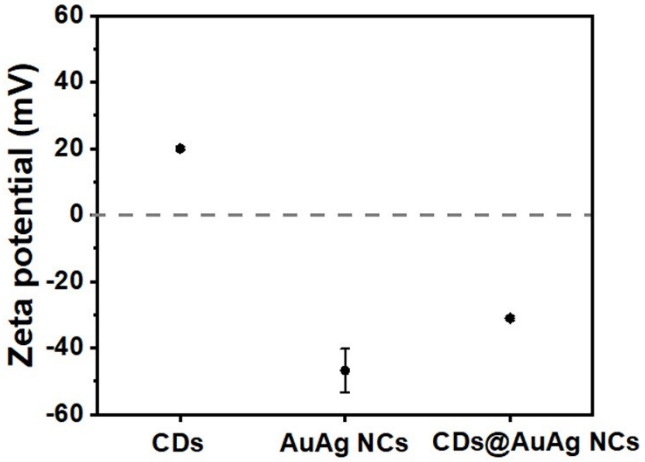

Figure S4. Zeta potentials of AuAg NCs, CDs and CDs@AuAg NCs (pH=6).

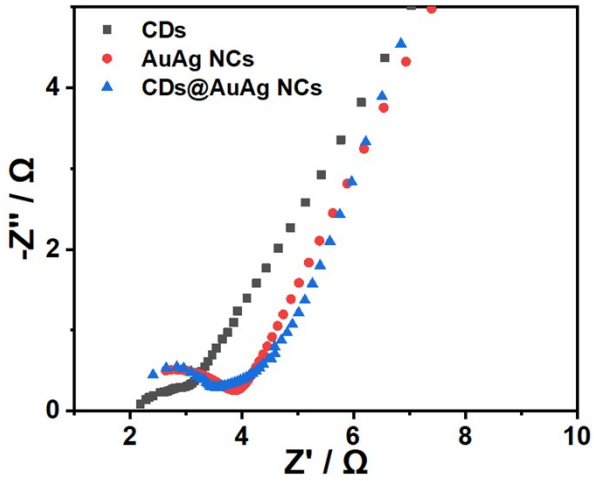

Figure S5. Nyquist plots of CDs, AuAg NCs and CDs@AuAg NCs.

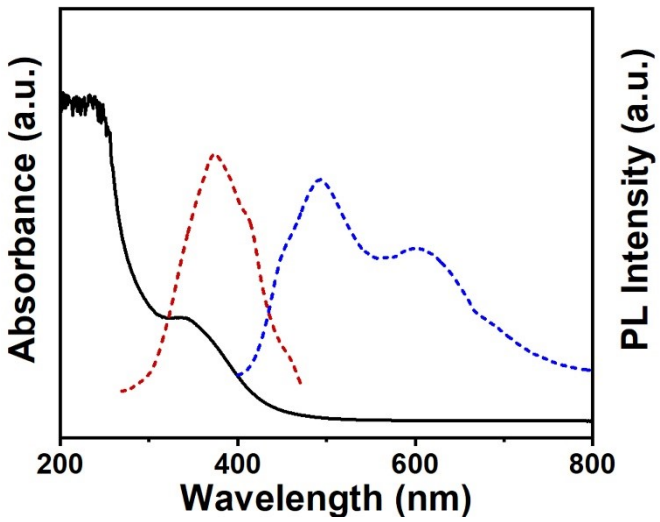

Figure S6. UV-visible absorption (black curve), photoexcitation (red curve), and photoemission spectra (blue curves) of CDs@AuAg NCs after 2 months storage at room temperature without visible-light illumination.

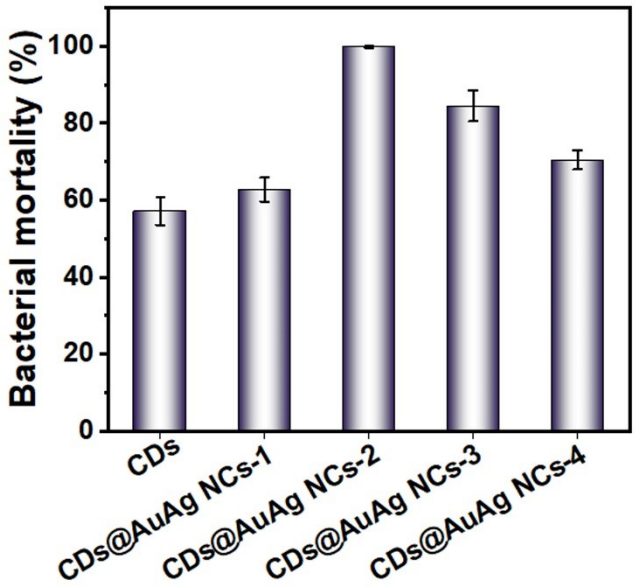

Figure S7. The antibacterial efficiencies of photodynamic antibacterial agent CDs@AuAg NCs-X with CDs as reference. (Note: X = 1, 2, 3 and 4, correspond to samples with different concentrations of the added AuAg NCs: 1 mM, 2 mM, 3 mM and 4 mM, respectively).

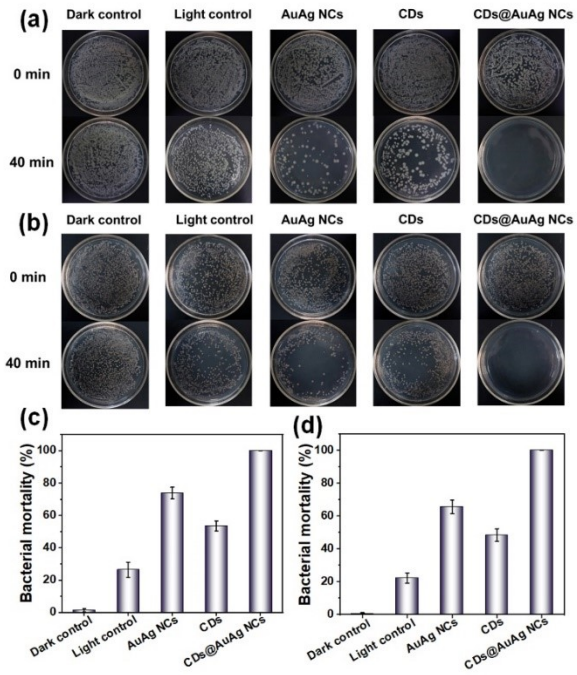

Figure S8. Bacterial colony growth of *B. subtilis* (a) and *P. aeruginosa* (b) in the presence of AuAg NCs, CDs, CDs@AuAg NCs, and water (as control) under visible-light illumination or dark condition for 40 min. Bacterial mortalities of *B. subtilis* (c) and *P. aeruginosa* (d) treated with corresponding samples under visible-light illumination or dark condition .

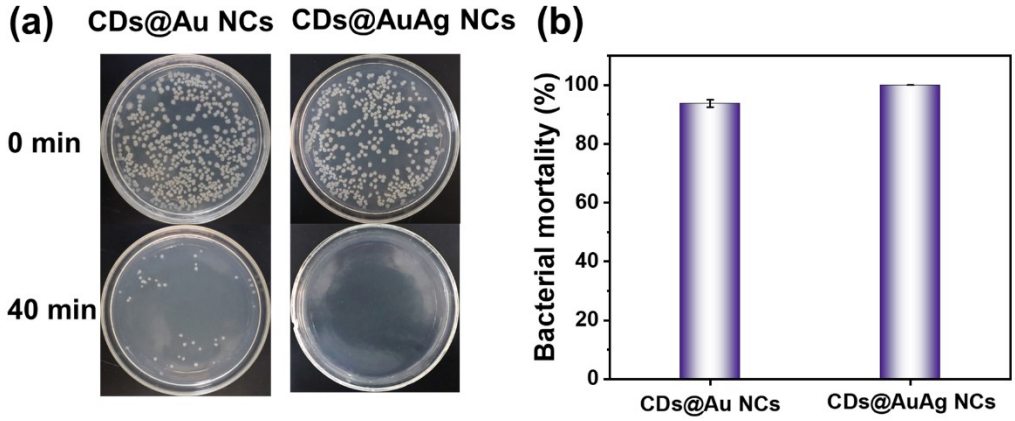

Figure S9. (a) Bacterial colony growth of *E. coli* in the presence of CDs@Au NCs and CDs@AuAg NCs under visible-light illumination for 40 min. (b) Bacterial mortalities of *E. coli* treated with CDs@Au NCs and CDs@AuAg NCs under visible-light illumination.

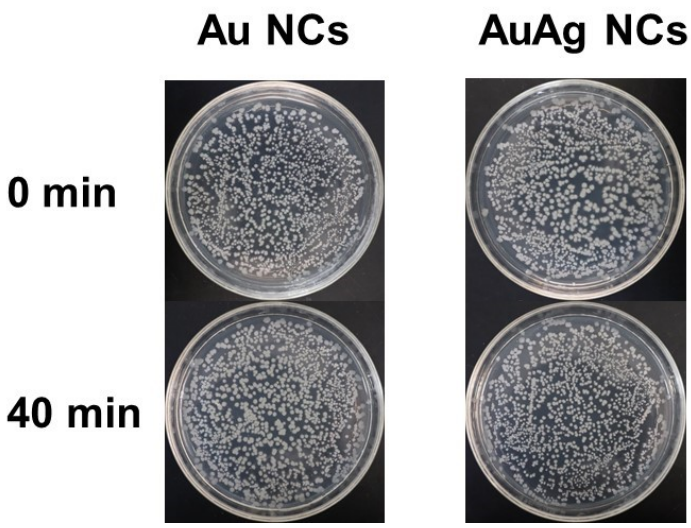

Figure S10. Bacteria colony growth of *E. coli* in the presence of Au NCs and AuAg NCs under dark condition for 40 min.

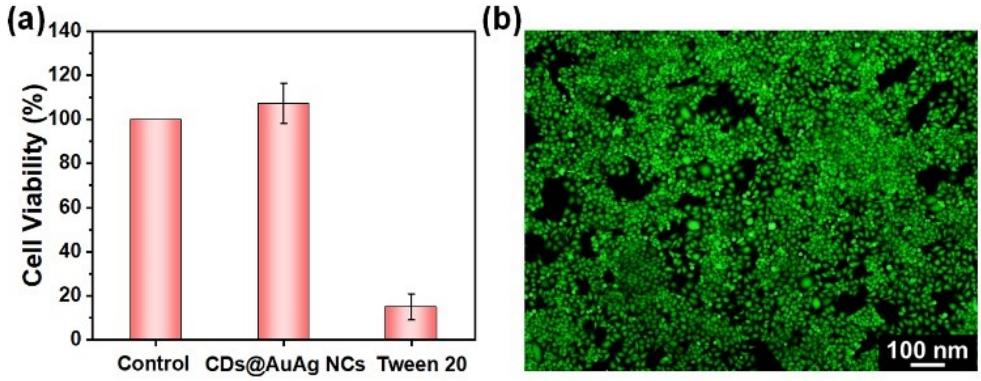

Figure S11. (a) Cytotoxicity assay of CDs@AuAg NCs, water (as negative control) and Tween 20 (as positive control) on HeLa cells evaluated by MTT Kit after 24 h treatment. (b) Fluorescence microscope image of viable cells stained with acetomethoxy derivate of calcein (green color) and nonviable cells stained with ethidium homodimer 1 (red) after 12 h treatment with CDs@AuAg NCs.

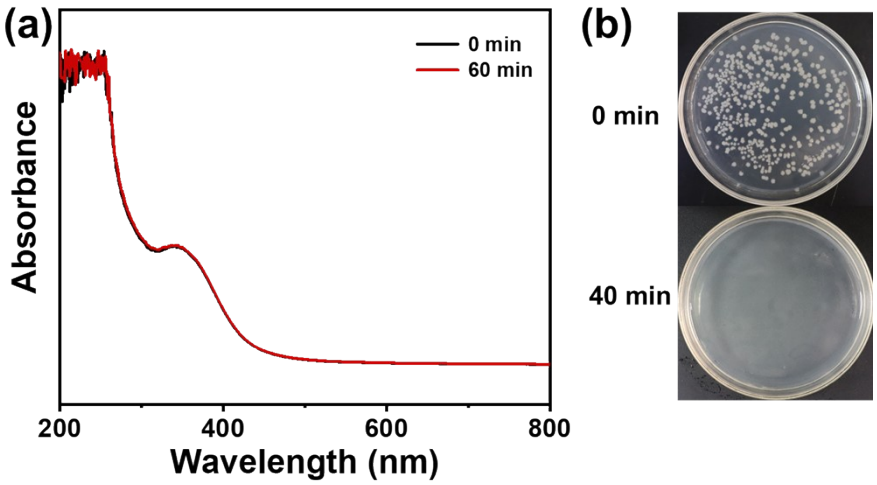

Figure S12. (a) The UV-visible absorption spectra of CDs@AuAg NCs before and after visible-light illumination for 60 min. (b) The photodynamic antibacterial activity of the CDs@AuAg NCs that being illuminated by visible light for 60 min.

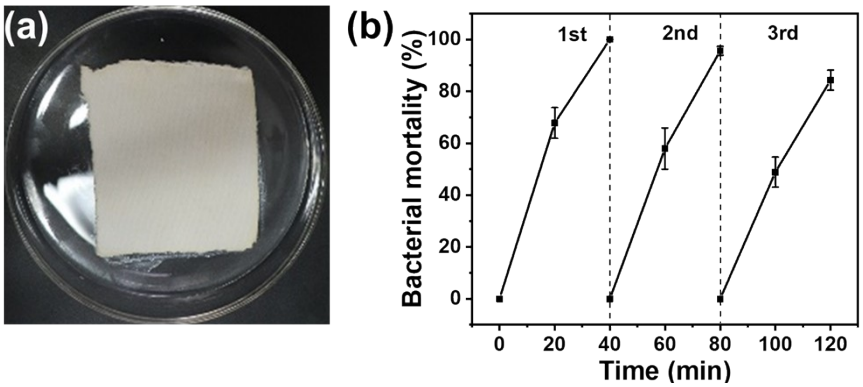

Figure S13. (a) Digital photo of CDs@AuAg NCs-functionalized antibacterial clothing. (b) The bactericidal efficacy of CDs@AuAg NCs-functionalized clothing with different cycles of antibacterial test.

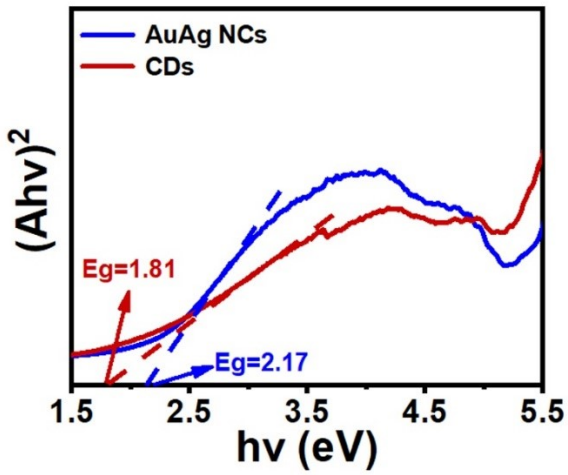

Figure S14. The calculated energy gap (Eg) of pristine AuAg NCs and CDs according to their corresponding UV-visible DRS.

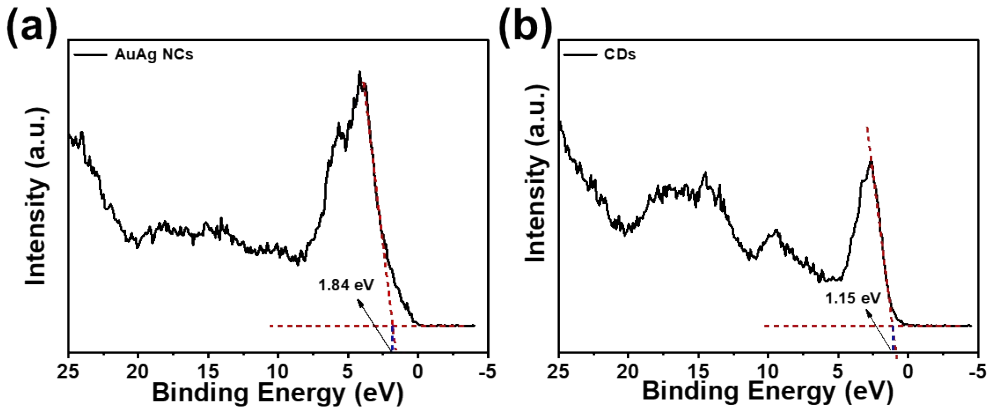

Figure S15. VB-XPS curves of AuAg NCs (a) and CDs (b).

Supplementary Note I: The VB potentials of AuAg NCs and CDs ($E_{VB\text{-}XPS}$) were measured as 1.84 V and 1.15 V according to their VB-XPS plots, respectively. Therefore, their VB values (V vs. NHE) were calculated to be 1.90 V and 1.21 V, respectively, based on the formula $E_{NHE} = \varphi + E_{VB\text{-}XPS} - 4.44$ (E_{NHE}: standard hydrogen electrode potential; φ: electron work function of the XPS analyzer, and the value was 4.50.).[1, 2] The CB position can be deduced from the equation, $E_{CB} = E_{VB} - E_g$ (E_g is the energy bandgap). On the basis of the above equations, the CB positions of AuAg NCs and CDs were calculated to be -0.27 V and -0.60 V, respectively.

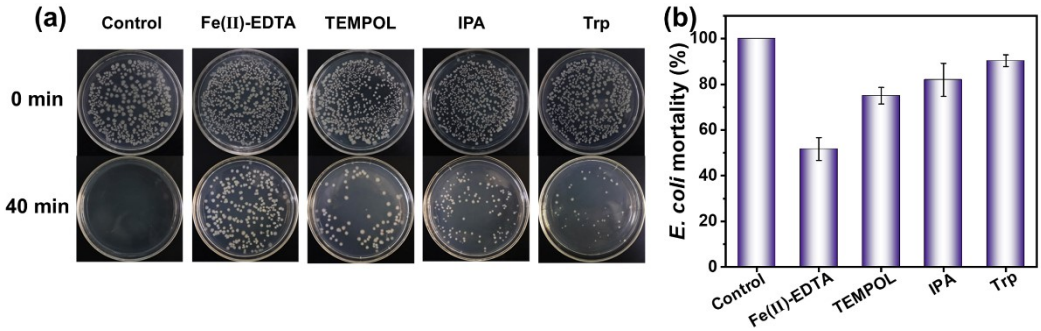

Figure S16. Bacterial colony growth (a) and the bacterial mortalities (b) of *E. coli* over CDs@AuAg NCs in the presence or absence of different scavengers.

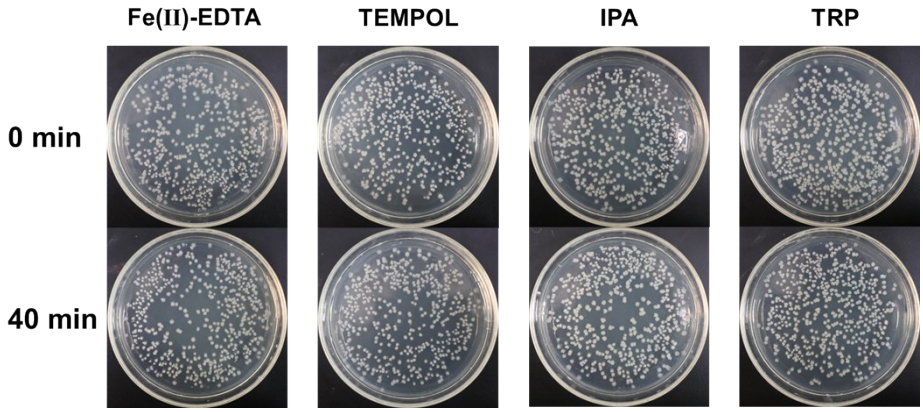

Figure S17. Bacteria colony growth of *E. coli* in the presence of Fe(II)-EDTA, TEMPOL, IPA and TRP.

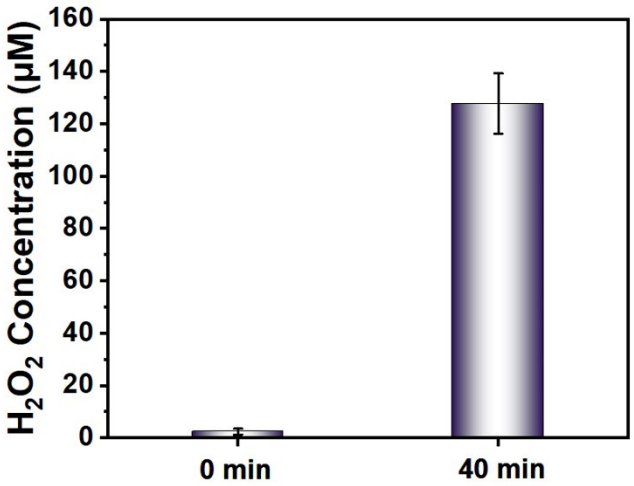

Figure S18. The H_2O_2 production over CDs@AuAg NCs under visible-light illumination for 40 min (H_2O_2 concentrations were determined by the quantitative peroxide assay kit).

Table S1. The fitting parameters for the PL decay curves of the CDs and CDs@AuAg NCs.

	τ_1 (ns)	τ_2 (ns)	τ_{ave} (ns)	$B_1/(B_1+B_2)$, %	$B_2/(B_1+B_2)$, %
CDs	1.50	9.76	8.67	49.85	50.15
CDs@AuAg NCs	1.30	8.08	6.64	62.64	37.36

References

1. J. Yuan, X. Liu, Y. Tang, Y. Zeng, L. Wang, S. Zhang, T. Cai, Y. Liu, S. Luo, Y. Pei and C. Liu, *Appl. Catal. B: Environ.*, 2018, **237**, 24-31.
2. J. Xiong, X. Li, J. Huang, X. Gao, Z. Chen, J. Liu, H. Li, B. Kang, W. Yao and Y. Zhu, *Appl. Catal. B: Environ.*, 2020, **266**, 118602.